Biomechanics of Coupled Motion in the Cervical Spine During Simulated Whiplash in Patients with Pre-existing Cervical or Lumbar Spinal Fusion: A Finite Element Study

by

Haoming Huang

Department of Biomedical Engineering
Duke University

Date:_____

Approved:

_____
Roger Nightingale, Supervisor

_____
Elizabeth Bucholz

_____
Zbigniew Kabala

_____

_____

Thesis submitted in partial fulfillment of the requirements
for the degree of Master of Science in the
Department of Biomedical Engineering in the
Graduate School of Duke University

2014

ABSTRACT

Biomechanics of Coupled Motion in the Cervical Spine During Simulated Whiplash in Patients with Pre-existing Cervical or Lumbar Spinal Fusion: A Finite Element Study

by

Haoming Huang

Department of Biomedical Engineering
Duke University

Date:_____
Approved:

_____
Roger Nightingale, Supervisor

_____
Elizabeth Bucholz

_____
Zbigniew Kabala

_____

_____

An abstract of a thesis submitted in partial fulfillment of the requirements
for the degree of Master of Science in the
Department of Biomedical Engineering in the
Graduate School of Duke University

2014

Abstract

It is well understood that loss of motion following spinal fusion increases strain in the adjacent motion segments. However, it is unclear if to date, studies on cervical spine biomechanics can be affected by the role of coupled motions in the lumbar spine. Accordingly, we investigated the biomechanics of the cervical spine following cervical fusion and lumbar fusion during simulated whiplash.

A validated whole-human finite element model was used to investigate whiplash injury. The cervical spine before and after spinal fusion was subjected to simulated whiplash exposure in accordance with Euro NCAP testing guidelines, and the strains in the anterior longitudinal ligaments of the adjacent motion segments were computed.

In the models of cervical arthrodesis, peak ALL strains were higher in the motion segments adjacent to the level of fusion, and strains directly increased with longer fusions. The mean strain increase in the motion segment immediately adjacent to the site of fusion from C2-C3 through C5-C6 was 26.1% and 50.8% following single- and two-level cervical fusion ($p=0.03$). On average, peak strains experienced in a lumbar-fused spine were 1.0% less than those seen in a healthy spine ($p=0.61$). The C3-C4 motion segment had disproportionately high increases in strain following cervical fusion. The C6-C7 motion segment experienced high absolute strain under all tested conditions but the increase in strain following fusion was very small. This study provides support for

both the hypothesis that adjacent segment disease is associated with post-arthrodesis biomechanical influences and the hypothesis that adjacent segment disease is a result of natural history, and inherent structures at risk.

Contents

List of Tables

List of Figures

1. Background

1.1 Significance

The objective of this thesis is to evaluate the biomechanics of the cervical spine following cervical and lumbar fusion in whiplash scenarios. Chapter 2 contains a manuscript titled "Biomechanics of Coupled Motion in the Cervical Spine During Simulated Whiplash in Patients with Pre-existing Cervical or Lumbar Spinal Fusion: A Finite Element Study" written for publication by H. Huang with co-authors R.W. Nightingale and A.C. Dang. With guidance and input from R.W. Nightingale and A.C. Dang, the study was designed and completed by H. Huang.

Chapter 1 provides an introduction to the relevant terms necessary to understand the discussions presented in the manuscript.

1.2 Relevant Terms

1.2.1 Spine Anatomy and Physiology

Henceforth, the standard anatomical directional terms shown in Figure 1 will be used to precisely communicate information about the human body and its constituent parts.

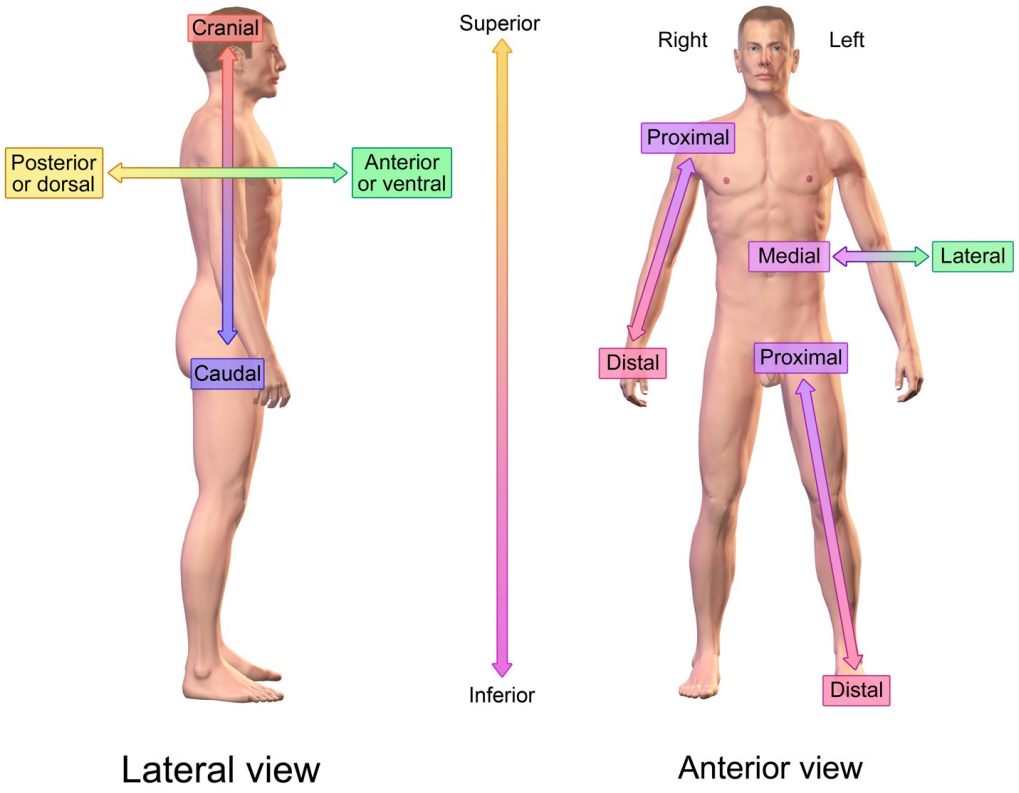

Figure 1: Standard Anatomical Directional References.[1]

The spine is generally described using four regions: the cervical, thoracic, lumbar, and sacral spine (Figure 2). The cervical spine (or neck) consists of 7 vertebral bodies (pieces of bone) named C1 to C7, with C1 as most superior and C7 as most inferior. Each adjacent body is separated by a layer of cartilage called an intervertebral disc. The boney features provide structure, protection, and a medium for calcium-exchange, while the cartilaginous components act as shock absorbers to prevent bone-on-bone contact. As with all bone in the human body, each vertebra consists of two parts: cortical (also known as compact) and trabecular (also known as cancellous or

spongy) bone. Cortical bone is the dense outer shell of bone, and trabecular bone is the porous interior of bone.

Although each vertebral body and intervertebral disc varies slightly in geometry, this model of alternating bone and cartilage is continuous throughout the thoracic and lumbar spine. The thoracic and lumbar spine consist of 12 and 5 vertebral bodies named T1—T12 and L1—L5, respectively. The sacral spine is unique in that it has 5 fused vertebral bodies named S1—S5. More commonly however, these fused bodies are referred to as a single unit: the sacrum. The coccyx (tailbone) is adjacent and immediately inferior to the sacrum, but should not be confused with S5.

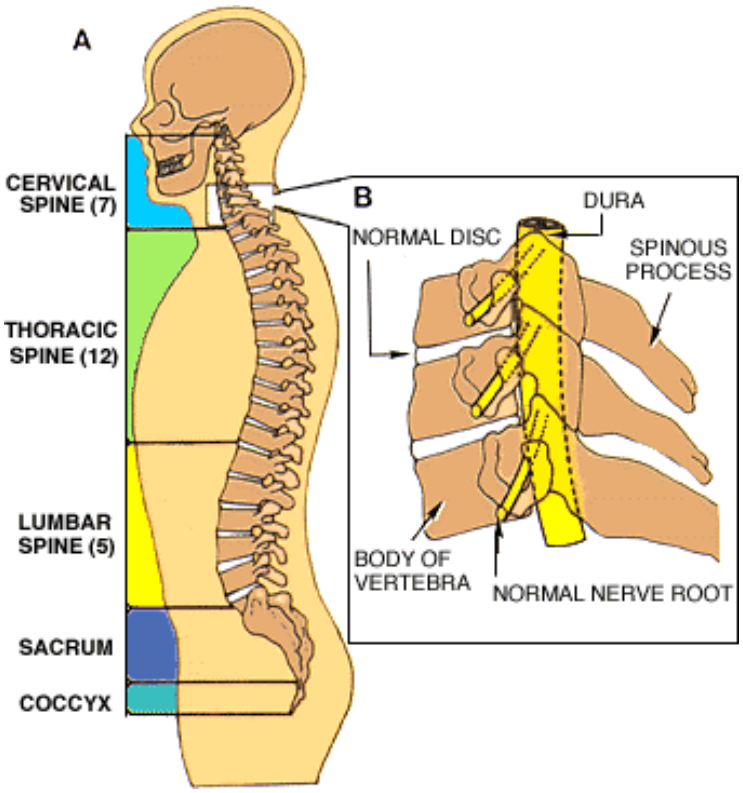

Figure 2: (A) Regions of the spine. (B) Enlargement of the cervical spine.[2]

In addition to bone and cartilage, several ligaments run down the length of the spine (Figure 3). These ligaments have functions such as providing spinal column stability during rest and normal movement, and limiting excessive motion caused by external circumstances such as car collisions. The anterior longitudinal ligament (ALL) and posterior longitudinal ligament (PLL) are two of the major spinal ligaments and limit extension and flexion, respectively. The ALL runs immediately anterior to the spine and the PLL runs immediately posterior to the spine. Both longitudinal ligaments run along the length of the spine from C2 to the sacrum.

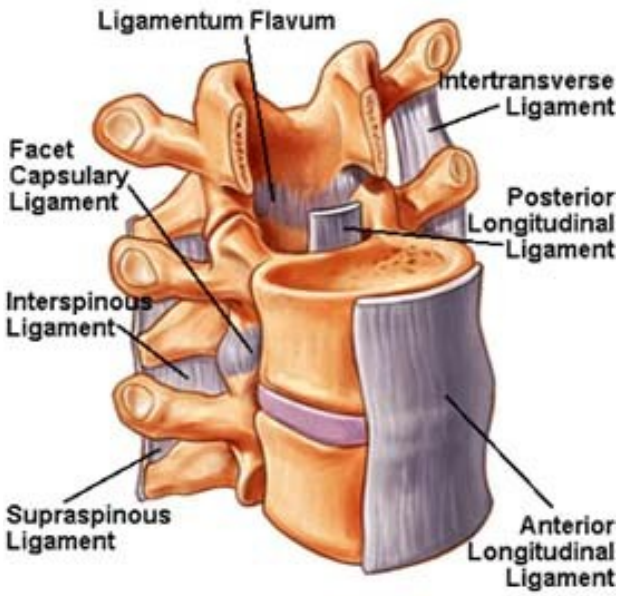

Figure 3: Spine ligaments.[3]

1.2.2 Clinical Terms

Spondylosis is a broad term that describes any patient who has both spinal degeneration and pain. Two of the most common areas of degeneration are in the facet

joints and intervertebral discs. If the degeneration is in the facet joints, the cause is likely osteoarthritis. If the degeneration is in the intervertebral discs, the cause is likely degenerative disc disease. The pain is typically a result of the compression of emerging spinal cord nerve roots when the gap between adjacent bodies narrows.

Our study focused on investigating the biomechanics of the cervical spine, and thus we are primarily interested in the causes of cervical spondylosis. Cervical spondylosis is generally attributed to an age-related degeneration of the discs.

Spinal fusion (also known as spinal arthrodesis or spondylodesis), is a surgical technique that fuses adjacent vertebrae by grafting supplementary bone tissue. Depending on the severity of spondylosis, one or more sets of vertebrae may be fused. For example, a single-level fusion such as C2—C3 fusion refers to surgically connecting the C2 and C3 vertebral bodies together. Likewise, a two-level C2—C4 fusion joins the C2, C3, and C4 bodies together.

There are several trade-offs with spinal arthrodesis. With each fusion, there is a trade-off between increased spinal stability and decreased spinal motion. This effect is particularly significant in the neck, because C2 acts as the primary axis for head rotation. For most of the spine, fusion results in restricted anterior-posterior movement. However, if C2 is ever fused, the loss of motion is amplified as the rotational degrees of freedom are limited as well. A second example of a trade-off of arthrodesis is adjacent segment disease. Adjacent segment disease refers to the deterioration of spinal levels

adjacent to the site of a previous fusion. It is unclear whether the complication is caused by undue stress placed on segments neighboring the fused spine, by natural spine aging, or by other reasons.

In the manuscript, we are interested in the effects of whiplash on strains in the cervical spine in patients who have previously undergone arthrodesis. Whiplash refers to a sudden neck flexion or extension (forward or rearward bending, respectively) that is particularly common in low-velocity (16 km/h) rear-impact vehicle collisions.

1.2.3 Computer Modeling Terms

The FEM (finite element method) is a numerical method that approximates solutions to systems of partial differential equations. The technique can efficiently solve extremely complex systems by discretizing large systems into smaller constituent pieces. Each piece is called an element, and 3 or more nodes define each element depending on the element type.

Benefits of FEM include accuracy, versatility, and reproducibility. The accuracy of the model can be easily improved by changing the mesh density (the number of elements that span a given area). Each increase in mesh density provides a more accurate estimate of the continuous solution at the expense of CPU runtime. Figure 4 shows an example of a mesh with higher density at the bottom left. The general idea is to use finer meshes for the parts of the model that are most critical to the analysis, and to use wider meshes for the remaining parts to minimize CPU runtime. The exceptions to

this rule will not be discussed in this thesis. In addition to high accuracy, FEM is versatile enough to be applied to nearly any application because each element can be defined uniquely in both section and material properties. Two commonly used section types include shell and solid elements. Two common material parameters include the Young's modulus and Poisson's ratio, just as examples. Lastly, a key benefit of using any mathematical model is that the results are consistently reproducible. Once a model has been validated, variables can be changed ad infinitum for the systematic testing of hypotheses.

Despite its numerous advantages, FEM does have its downfalls. One primary downfall is that the accuracy of the model is largely dictated by the materials selected for each part (group of similar elements). This material-dependent accuracy is particularly important when modeling human tissue because biological tissues often behave in extremely complex manners that are not easily described via traditional engineering material definitions. As a consequence of the inherent complexity of tissues, FEM can only act as an approximation of the system, with accuracy as a function of how well the tissues are represented.

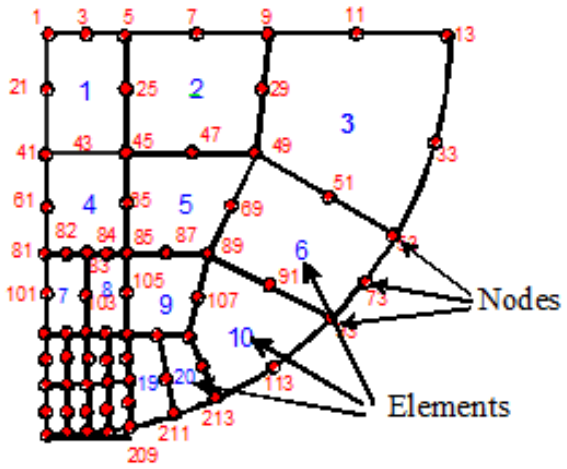

Figure 4: A mesh is comprised of elements and nodes.[4]

In our study, we simulated a rear-impact vehicle collision by loading a validated whole-human FEM model. We quantified the differences in cervical spine ALL strain in a healthy spine versus a fused spine, in realistic whiplash scenarios. Figure 5 shows the geometry of the cervical spine in the FEM model that was used. The ALL segments were represented as shell elements and are highlighted; the mesh outline was removed for easier viewing. The numbered nodes on each ALL segment were used to measure the strain. Strain was defined as the change in distance between each pair of nodes, divided by the original distance.

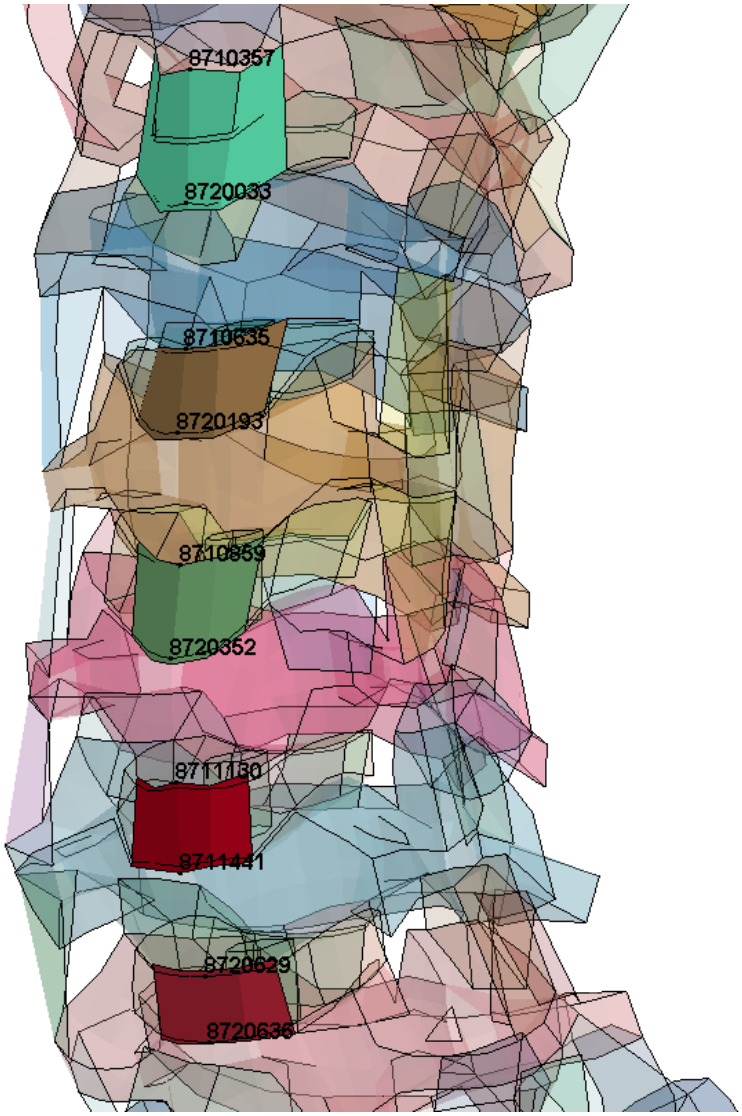

Figure 5: A finite element model of the cervical spine. The five highlighted parts represent the ALL segments corresponding to the C1 (top) through C5 (bottom) vertebrae. The mesh has been hidden for viewing purposes.

2. Effects of Fusions on Strains in the ALL in Whiplash Exposures

2.1 Introduction

Whiplash injuries, caused by a sudden or unexpected neck flexion or extension, are the most frequently reported injury in low-velocity rear-impact vehicle collisions today.[5] The economic impact related to whiplash injury is estimated to be as high as $3.9 billion annually in the United States, or more than $29 billion when litigation costs are considered.[6] Some of the challenges of whiplash are the associated secondary gain that may confound injury[6], associated non-organic signs of disability[6], and the difficulty of establishing consistent MRI findings for diagnosis.[7] Nonetheless, large defined population studies have shown that the incidence of patients presenting to the hospital with whiplash related complaints may increase even when a concomitant *decrease* in insurance claims is observed.[8] Additionally, the overall body of literature provides evidence supporting a lesion-based model of whiplash injury.[9] Injury to the anterior longitudinal ligament (ALL) appears to be a marker to severe whiplash injuries in both cadaveric studies[10] and post-mortem studies.[11,12]

The majority of studies on whiplash have focused on patients with no pre-existing cervical spine disease. Cervical spine arthrodesis is a common procedure with over 1.1 million estimated patients undergoing the procedure over an 8 year period in the United States alone.[13] The effects of cervical arthrodesis on the adjacent motion segments above and below the level of fusion still remain a point of debate. It is clear

that there is increased strain in the soft tissue and vertebrae in adjacent motion segments due to compensation for the new loss of flexibility.[14,15] However, motion sparing procedures such as cervical disc arthroplasty have failed to show decreased rates of adjacent segment disease, at least for single level surgery.[16]

We have previously quantified the biomechanical effects of an 8g whiplash following cervical arthrodesis on adjacent segment strains seen in the ALL using a validated finite element (FE) model.[15] To better understand both adjacent segment biomechanics and cervical spine biomechanics, we sought to study the potential coupled motions between the cervical and lumbar spine and also addressed two limitations from our prior work.

In our original study, the impact scenario selected was based upon whole cadaver experiments performed by Mertz[17] in 1967 and whole cervical spine model experiments performed by Ivancic[18] in 2004 reflecting an 8g peak acceleration. Though those historical impact pulses provided a method for validation and assessment of failure, newer data is available that reflects more realistic real-world, rear-impact collisions.[5] We sought to study cervical spine biomechanics after spinal fusion using the low-speed acceleration pulses described by the European New Car Assessment Programme (Euro NCAP). Other popular testing organizations, including the US National Highway Traffic Safety Administration (NHTSA) and the private Insurance Institute for Highway Safety (IIHS), do not have rear-impact whiplash standards in their

testing. Additionally, our prior study used a simplified FE model of the whole cervical spine and did not capture the additional effects caused by coupled motions from the lumbar spine, nor the effects created by the interaction between the model and the driver's seat. Advances in computational resources have allowed us to address these limitations and test the hypothesis that there would be significant differences in ALL strains between our prior methodology and simulations implementing a realistic seat and torso interaction.

We sought to provide quantitative data on the potential effects of adjacent segment strains following cervical and lumbar arthrodesis as well as gain an increased understanding of the biomechanics of the post-operative cervical spine with fused segments during a realistic whiplash scenario. We hypothesized that lumbar arthrodesis would not significantly affect the cervical strains seen in whiplash due to the relatively long distance between the cervical and lumbar spines.

2.2 Materials and Methods

2.2.1 Finite Element Model Overview

THUMS (Total Human Model for Safety [Occupant Model v1.61, Toyota Central Research & Development Labs, Nagakute, Japan]), a 3-dimensional FE model of a 75 kg, 175 cm tall, 35-year-old male seated in a driving position, was used as the baseline for our whiplash simulations. THUMS incorporates roughly 91,200 total elements, 7,000 of which represent the cervical spine, and 15,500 of which for the remaining thoracic and

lumbar spine. The spongy and cortical bone of the vertebral bodies were modeled as rigid solid and shell entities, respectively. The intervertebral discs were modeled using a combination of solid (pulposus and annulus) and seatbelt (lamellae) elements with isotropic material and section properties. The ALL, posterior longitudinal ligament (PLL), and other ligaments including the ligamentum flavum, ligamentum nuchae, and intertransverse ligament were represented using 2-dimensional shell elements, assigned with varying unique material properties. Only the deep layers of the ALL and PLL were modeled. All solid and shell elements in the cervical spine were defined as isotropic, linear elastic materials. Muscles were represented using Hill-type muscle models each comprised of two non-linear spring elements, a contractile element, and a viscous damper to address muscle viscoelasticity. Muscles and ligaments were allowed to react freely to applied loads, but no active muscle and ligament forces were incorporated into the model. The THUMS model has been previously validated as a computational tool to quantify both local and global spine kinematics.[15,19]

All FE calculations were run using single-precision LS-DYNA R701 64-bit (Livermore Software Technology Corp., Livermore, CA) on a Microsoft Windows workstation (Core i5-3570k "Ivy Bridge", Intel Corp., Santa Clara, CA; Z77 Extreme4 ATX, ASRock Inc. Taipei, Taiwan; BLS8G3D1609DS1S00, Micron Technology Inc., Boise, ID; Radeon HD7870 GHz Edition 2GB, Sapphire Technology Limited, Hong Kong, China). LS-PrePost 3.2 64-bit (Livermore Software Technology Corp., Livermore, CA),

Excel 2013 (Microsoft Corp., Redmond, WA), and MATLAB 7.12.0.635 64-bit (MathWorks Inc., Natick, MA) were used to pre-process, post-process, and analyze the data. GraphPad 6.0 (GraphPad Software, La Jolla, CA) was used for statistical analysis. Unpaired two-way Student t-tests were used to compare *change* in adjacent segment ALL strain following different cervical arthrodesis procedures. Paired two-way Student t-tests were used to compare ALL strain and change in ALL strain in specific motion segments following different modeling conditions. A two-way analysis-of-variance (ANOVA) with Tukey post-test was used to compare *change* in cervical ALL strain following different thoracolumbar arthrodesis procedures.

2.2.2 Virtual Surgery Overview

All cervical and lumbar fusions were assumed to be complete and fully healed. This was simulated by rigidly constraining the cortical and spongy elements of adjacent vertebral bodies to one another. Instrumentation was not simulated in our model.

Single-level cervical arthrodesis was modeled by constraining C2-C3, C3-C4, C4-C5, C5-C6, and C6-C7. Two-level cervical arthrodesis was assumed contiguous and modeled by constraining C2-C4, C3-C5, C4-C6, and C5-C7. ALL strains were evaluated at the neighboring adjacent motion segments one- and two-levels away from the cervical fusion site. For instance, in the C4-C5 fusion case, the segments one-level away were defined as ALL segments C3-C4 and C5-C6. The segments two-levels away are defined as ALL segments C2-C3 and C6-C7.

THUMS assumes that the entire sacral spine is fused and does not incorporate separate elements to differentiate S1 through S5. As such, L5-S1 arthrodesis was modeled by constraining L5 to the sacrum. L2-L5 arthrodesis was modeled by constraining L2-L3, L3-L4, and L4-L5. L2-S1 arthrodesis was modeled by constraining L2-L3, L3-L4, L4-L5, and L5-sacrum. Lastly, T9-S1 arthrodesis was modeled by constraining T9-T10, T10-T11, T11-T12, T12-L1, L1-L2, L2-L3, L3-L4, L4-L5, and L5-sacrum. Lumbar fusion was performed without alteration of the sagittal alignment of the model. Strains for the lumbar test cases were evaluated at ALL segments C2-C3, C3-C4, C4-C5, C5-C6, and C6-C7.

2.2.3 Loading Conditions

Whiplash exposures were simulated by applying a 16 km/h ΔV, 10g peak acceleration, 92 ms duration, triangular-shaped load curve to the model. This curve, defined and used by Euro NCAP as well as the International Insurance Whiplash Prevention Group (IIWPG), is representative of whiplash-inducing accidents.[5,20] Loads were applied to the model in two different ways: "T1 Acceleration" and "Seat Interaction".

T1 Acceleration Model: In the first set of simulations, all nodes at or below the T1 vertebrae in the FE model were treated as a rigid body and loaded with the above described Euro NCAP pulse in the posterior to anterior x-direction. The load was removed after it had run the full 92 ms duration and the model was allowed to continue

its inertial movement until the termination of the simulation at 300 ms. Data was outputted at 2.5 ms time intervals throughout the length of the simulation. This simulates the cervical spine and head in isolation and the contribution of the coupled motions of the lumbar spine are not considered.

Seat Interaction Model: In the second set of simulations, a seat and floor were added using rigid 4-by-4 element shells via LS-PrePost to the baseline THUMS model. The seat was defined as two separate parts: a seat back and a seat bottom. The seat angle was fit to the curvature of our validated FE model, and in accordance with the angles described in SAE J826 H-point manikins fitted with a Head Restraint Measuring Device and the Euro NCAP whiplash testing protocol.[21,22]

Initially, the seat and floor were fixed in all 6 degrees of freedom (x-, y-, z- translational and x-, y-, z- rotational) and positioned 1 mm below the THUMS model. Gravity was then applied for 3 seconds to relax the THUMS model into the seat in preparation for the ensuing whiplash exposure. Whiplash was again simulated as described above. Data was outputted every 2.5 ms. The FE model with the added seat and floor is shown in Figure 6.

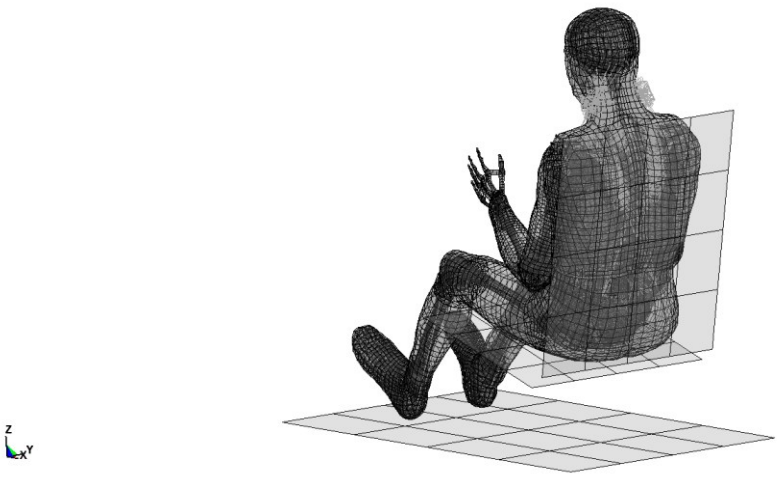

Figure 6: The validated FE model with a rigid seat and floor shown using a semi-transparent filter.

2.3 Results

Representative snapshot images of the whiplash simulation are in Figure 7. Figure 8 compares the differences in resultant head acceleration between the T1 Acceleration Model and the Seat Interaction model. The T1 Acceleration Model showed a 10g increase and 8 ms phase delay in peak head acceleration.

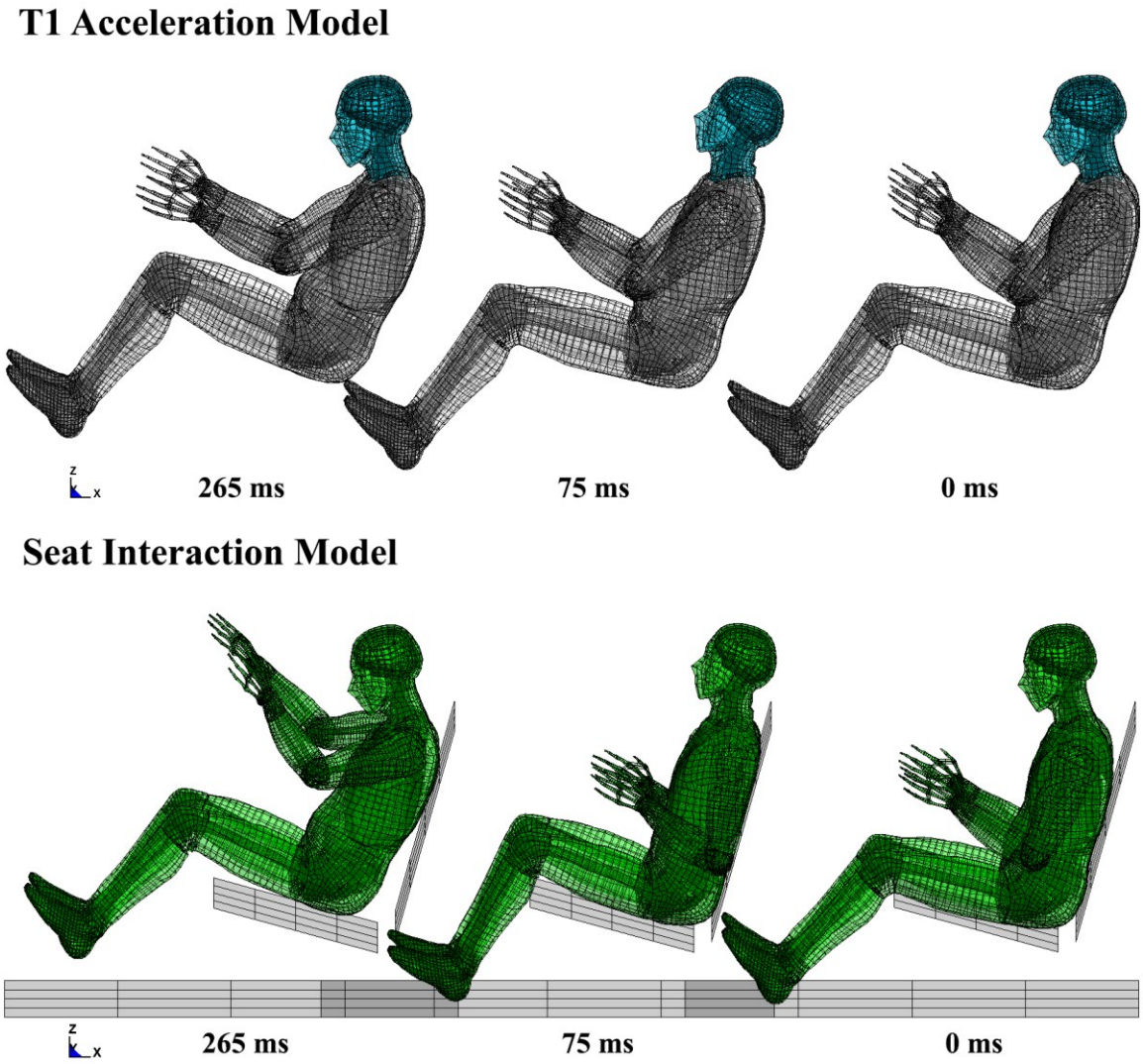

Figure 7: Snapshots of the T1 Acceleration Model and the Seat Interaction Model. At 0 ms in the T1 Acceleration Model, a 16 kilometer per hour pulse with a 10g peak acceleration is applied, leftward, to all dummy nodes at or below the T1 vertebrae. By 75 ms, the majority of the load has been applied. By 265 ms, all of the load has been applied and the dummy is moving forward at a constant velocity. At 0 ms in the Seat Interaction Model, the same pulse is applied leftward to the rigid seat. At 75 ms, the seat is slightly past mid-impact with the dummy. By 265 ms, the impact is complete resulting in the dummy separating from the seat.

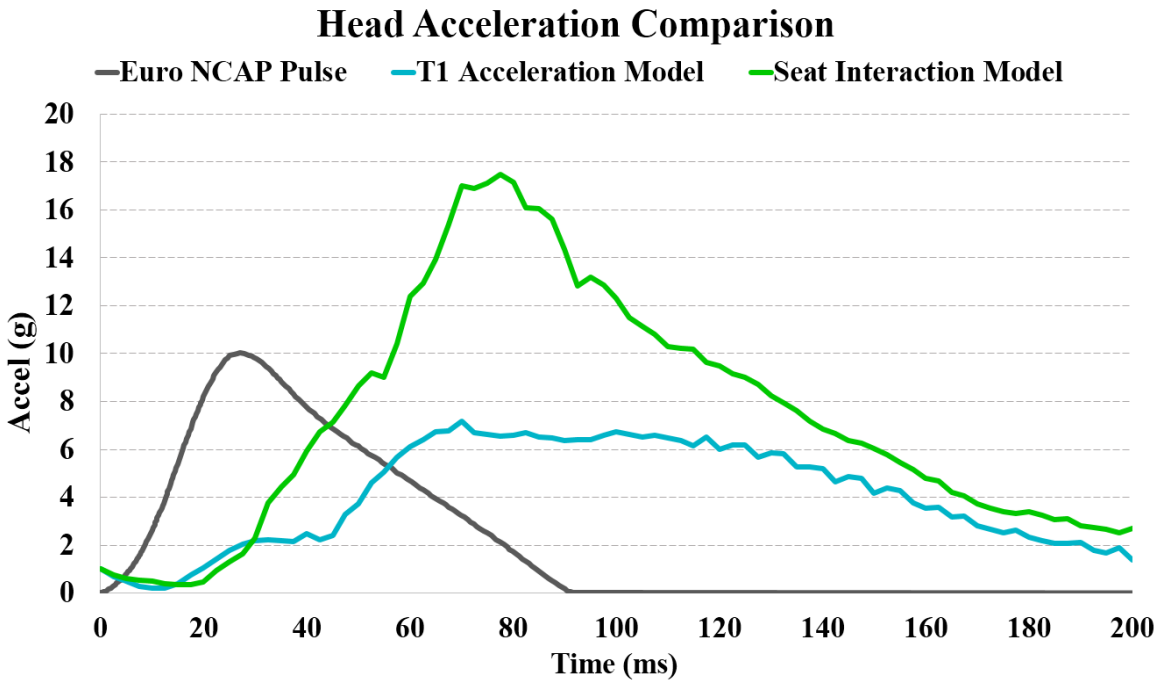

Figure 8: Comparison of resultant head accelerations in two models loaded using the same Euro NCAP pulse. The T1 Acceleration Model experienced a 7.2g peak head acceleration at 70 ms. The Seat Interaction Model experienced a 17.5g peak head acceleration at 78 ms. A 5-point averaging filter was applied to the Seat Interaction Model curve to smooth out short-term fluctuations.

T1 Acceleration Model: An increase in ALL strain was seen for all fusion conditions. (Table 1). ALL strain in the baseline model ranged from 0.081 to 0.304, increasing from cranial to caudal levels. With the exception of C6-C7, ALL strain increased at all levels and ranged from 0.085 to 0.309. The C6-C7 motion segment experienced the smallest increase in strain of 0.58±0.78% (mean±SD) and seemed relatively unaffected, even by adjacent level fusion. The C3-C4 segment saw the greatest change of 47% following C4-C5 fusion. In the motion segments from C3-C6, the greatest increase in strain was seen with a single level fusion at the level immediately below the

site of fusion. That is, C3-C4 ALL strain was greater following C4-C5 fusion as opposed to C2-C3 fusion and C4-C5 ALL strain was greater following C5-C6 fusion as opposed to C3-C4 fusion. Following two-level cervical fusion, ALL strain ranged from 0.099 to 0.322. At individual motion segments, the C6-C7 motion segment saw the least change in strain of 2.5±3.0% while again, C3-C4 saw the greatest increases in strain of 79.1±38.1%. When analyzed in aggregate, the change in adjacent segment strain was 23.0±13.9% for single-level fusion and 49.8±33.1% for two-level fusion ($p = 0.056$). If C6-C7 is removed from the statistical analysis, the change in adjacent segment strain in C2 through C6 was 26.0±11.8% for single level fusion and 58.6±28.1% for two-level fusion ($p = 0.019$).

Table 1: Peak strain of the anterior longitudinal ligament (ALL) increased following spinal fusion. The ALL at C3-C4 following C4-C5 fusion and C4-C6 fusion had the greatest change in strain for single- and two-level fusion, respectively. Although absolute strain was highest as C6-C7, this level experienced the least amount of change following fusion. The difference in adjacent segment strain in C2-C3 to C5-C6 between single- and two-level fusion was significant (p = 0.019).

	Baseline	Single-Level Fusion					2-Level Fusion			
ALL Segment		C2-C3 Fusion	C3-C4 Fusion	C4-C5 Fusion	C5-C6 Fusion	C6-C7 Fusion	C2-C4 Fusion	C3-C5 Fusion	C4-C6 Fusion	C5-C7 Fusion
C2-C3	0.081		0.092 (13.6%)	0.099 (22.2%)	0.091 (12.3%)	0.085 (4.9%)		0.126 (55.6%)	0.122 (50.6%)	0.099 (22.2%)
C3-C4	0.117	0.133 (13.7%)		**0.172 (47.0%)**	0.148 (26.5%)	0.150 (28.2%)			**0.241 (106.0%)**	0.178 (52.1%)
C4-C5	0.169	0.187 (10.7%)	0.201 (18.9%)		0.22 (30.2%)	0.196 (16.0%)	0.223 (32.0%)			0.246 (45.6%)
C5-C6	0.180	0.187 (3.9%)	0.197 (9.4%)	0.232 (28.9%)		0.234 (30.0%)	0.208 (15.6%)	0.277 (53.9%)		
C6-C7	0.304	0.304 (0.0%)	0.304 (0.0%)	0.306 (0.7%)	0.309 (1.6%)		0.305 (0.3%)	0.308 (1.3%)	0.322 (5.9%)	

Seat Interaction Model. An increase in ALL strain was seen under all conditions. (Table 2). ALL strain ranged from 0.106 to 0.382 in our model, increasing from cranial to caudal levels. Following single-level fusion, ALL strain ranged from 0.116 to 0.398. At individual motion segments, the C6-C7 motion segment experienced the least change in strain of 1.51±1.87% following all tested single-level fusion conditions while C3-C4 saw the greatest change of 42.8% following C4-C5 fusion. In the motion segments from C2-C5, the greatest increase in strain was seen with a single level fusion at the level immediately below the site of fusion. Following two-level cervical fusion, ALL strain ranged from 0.132 to 0.399. At individual motion segments, C6-C7 motion segment saw

the least change in strain of 3.3±1.7% while again, C3-C4 saw the greatest increases in strain of 71.3±15.1%. When analyzed in aggregate, the change in adjacent segment strain following single level fusion was 23.4±13.8% and it was 43.1±27.4% following two-level fusion ($p = 0.10$). If C6-C7 is removed from the statistical analysis, the change in adjacent segment strain in C2-C3 through C5-C6 following single level fusion was 26.1±12.3% and it was 50.8±22.2% following two-level fusion ($p = 0.03$).

Table 2: Peak strain of the anterior longitudinal ligament (ALL) increased following spinal fusion. The ALL at C3-C4 following C4-C5 fusion and C4-C6 fusion had the greatest change in strain for single- and two-level fusion, respectively. Absolute strain was generally higher in the Seat Interaction Model compared to the T1 Acceleration Model. Although absolute strain was highest as C6-C7, this level experienced the least amount of change following fusion. The difference in adjacent segment strain in C2-C3 to C5-C6 between single- and two-level fusion was significant ($p = 0.03$).

	Baseline	Single-Level Fusion					2-Level Fusion			
ALL Segment		C2-C3 Fusion	C3-C4 Fusion	C4-C5 Fusion	C5-C6 Fusion	C6-C7 Fusion	C2-C4 Fusion	C3-C5 Fusion	C4-C6 Fusion	C5-C7 Fusion
C2-C3	0.106		0.132 (24.5%)	0.127 (19.8%)	0.122 (15.1%)	0.116 (9.4%)		0.170 (60.4%)	0.142 (34.0%)	0.132 (24.5%)
C3-C4	0.145	0.162 (11.7%)		**0.207 (42.8%)**	0.194 (33.8%)	0.157 (8.3%)			**0.264 (82.1%)**	0.233 (60.7%)
C4-C5	0.202	0.224 (10.9%)	0.223 (10.4%)		0.264 (30.7%)	0.197 (-2.5%)	0.255 (26.2%)			0.270 (33.7%)
C5-C6	0.209	0.225 (7.7%)	0.243 (16.3%)	0.289 (38.3%)		0.260 (24.4%)	0.272 (30.1%)	0.317 (51.7%)		
C6-C7	0.382	0.384 (0.5%)	0.382 (0.0%)	0.387 (1.3%)	0.398 (4.2%)		0.387 (1.3%)	0.398 (4.2%)	0.399 (4.5%)	

Lumbar fusion had no meaningful impact in cervical spine strain with an average change of -1.0±4.1% strain (Table 3). No apparent pattern could be recognized

when evaluating a single level lumbar fusion to a complete thoracolumbar fusion (p = 0.61).

Table 3: Lumbar fusion had minimal impact in cervical spine strain and change in strain. The average change for all tested conditions was -1.0% strain (4.1% SD). There was no difference in change when comparing a single level lumbar fusion at L5-S1 to a thoracolumbar fusion from T9-S1 (p = 0.61).

ALL Segment	Baseline	L5-S1 Fusion	L2-L5 Fusion	L2-S1 Fusion	T9-S1 Fusion
C2-C3	0.106	0.107 (0.9%)	0.107 (0.9%)	0.106 (0.0%)	0.111 (4.7%)
C3-C4	0.145	0.137 (-5.5%)	0.134 (-7.6%)	0.135 (-6.9%)	0.136 (-6.2%)
C4-C5	0.202	0.203 (0.5%)	0.202 (0.0%)	0.203 (0.5%)	0.179 (-11.4%)
C5-C6	0.209	0.215 (2.9%)	0.212 (1.4%)	0.214 (2.4%)	0.209 (0.0%)
C6-C7	0.382	0.382 (0.0%)	0.384 (0.5%)	0.385 (0.8%)	0.385 (0.8%)

Comparisons between models: Modeling the whole human with seat interaction generated an average of a 23.0% increase in ALL strain (9.5% SD single level fusion; 8.3% SD two level fusion; both $p < 0.0001$). However, when comparing *change* in strain following single-level fusion, adding the seat interaction did not result in a significant difference (–0.5±7.5%; p = 0.76 and –0.2±10.1%; p = 0.48). The CPU runtime ranged from 4 to 7 hours per simulation. The runtime varied with two factors: CPU load and the number of cores used per simulation.

2.4 Discussion

A validated complete human FE model was updated to investigate the effects of cervical and lumbar fusions on peak ALL strains seen in the neck under a realistic whiplash impact pulse with the addition of a rigid car seat and floor. The model that included a seat interaction resulted in a significant 23% increase in the ALL strains, which indicates that the seat interaction is important in injury prediction. However, there was no significant difference in the way the models assessed the changes in ALL strain with fusion, suggesting that the more computationally efficient T1 Acceleration Model may be adequate to quantify these effects.

Increase in ALL strain was seen following all cervical spine procedures and statistically significant increases in ALL strain between one- and two-level fusions were seen in both the T1 Acceleration Model and Seat Interaction Model ($p = 0.019$ and $p = 0.03$, respectively) when analyzing the motion segments between C2-C6. C6-C7 showed relatively high levels of ALL strain under all tested conditions including the baseline, non-operative condition. Our strain of 0.3 in the baseline model was close to the tolerance of the ALL according to Yoganandan[23], but well below the 0.8 from the dynamic tests of Bass.[24] The addition of a seat back increased specific values of ALL strain by 23.0% ($p < 0.0001$). However, the percent change in ALL strain following surgery remained consistent for all conditions ($p = 0.76$ for single-level and $p = 0.48$ for two-level fusion). This reconfirms that our model is robust in its assessment in change of

tissue level adjacent segment ALL strain following cervical fusion under a broad range of conditions. We believe that the increased strain in the whole-human test condition was likely a result of the additional shorter impulse delivered to the neck due to the decoupling of the body from the seat and the vertical acceleration component from straightening of the compliant lumbar and thoracic spines. Additionally, the presence of soft-tissue interactions surrounding the muscle elements may have further contributed to the larger strains to the cervical spine. Lumbar fusion had no meaningful effect on cervical strain (-1.0% change, $p = 0.61$).

Several interesting clinical conclusions can be made from this data. Modern reports of adjacent segment disease have indicated that C4-C5 and C6-C7 are the two levels most affected by adjacent segment disease, potentially reflecting changes in technique.[25] Additionally, plate distance from the vertebral endplate has also been shown to affect adjacent segment ossification.[26] Our data shows that C6-C7 experiences the highest strain at baseline and that single-level cervical fusion did not appear to have meaningful difference in biomechanical strain. In contrast, C3-C4, which under normal conditions experiences lower ALL strain under these conditions and is infrequently a treated motion segment in isolation, experienced the largest increases in cervical ALL strain following arthrodesis in comparison to the other motion segments. Thus our data is in agreement with the current theory that adjacent segment disease reflects both the natural history of cervical spondylosis (C6-C7) as well as biomechanical factors (C3-C4).

It would be worthwhile in the future to re-evaluate data from cervical disc arthroplasty, which has yet to demonstrate decreased adjacent segment disease, with this in mind. Perhaps, motion sparing surgery at C4-C5 will have advantages over fusion when considering adjacent disease at C3-C4.

Second, lumbar fusion does not appear to have any meaningful impact in the cervical spine during whiplash. This supports our hypothesis. A claim that neck symptoms have been exacerbated by prior lumbar fusion in the absence of sagittal imbalance is not supported by the data generated in this study.

Complete ALL failure has been documented to occur at threshold strains between 0.426 and 0.476[23], with partial injury occurring at strains above 0.222.[18] Our results suggest partial injury during whiplash to the ALL at the C6-C7 level for a patient with a normal, unfused spine. Patients who have undergone fusion appear to have an increased risk of injury. In the majority of our simulations, one or more ALL segments would have reached partial failure thresholds following surgery. Thus it would be prudent to consider the relative risks and benefits of motion sparing alternatives for patients needing cervical spine operations.

Several limitations exist for future consideration but do not affect the conclusions drawn above. In real-world vehicle collisions, muscles and ligaments contract either in anticipation or as an instantaneous response to the impact. These could either exacerbate of alleviate these strains depending on the subject dependent muscle activations.[27,28]

Differences in strain were identified between our T1 Acceleration and Seat Interaction conditions. Though a realistic whiplash impulse was used, our data cannot be applied directly in a forensic situation as our seat is rigid and based on the geometry in the SAE J826 standard. Our seat did not include a head rest or incorporate the whiplash prevention and mitigation technologies currently found in most vehicles. A final limitation is that the etiology of whiplash syndrome may involve the facet capsules.[29,30] Unfortunately, the capsules are not modeled with sufficient fidelity in v1.61 of the THUMS model for a confident strain analysis. However, these limitations do not change the points made in this study.

3. Effects of Pulse Shape on Strains in the ALL

3.1 Introduction

To further support the validity of the methods employed in the above study, we sought to justify the triangular-shaped Euro NCAP pulse used in our model. We hypothesized that pulse shape does not affect cervical spine ALL strain given a fixed ΔV and fixed time interval when the pulse is applied directly to the nodes at or below the T1 vertebrae. However, when the same pulse is applied to the vehicle seat and indirectly transferred to the body, we hypothesized that there would be differences in the resulting ALL strain.

3.2 Materials and Methods

The same baseline total-human FE model used in chapter 2 was employed to simulate three new loading conditions: T1 acceleration frontal impact, T1 acceleration rear impact, and seat interaction. Strains were evaluated in a healthy, unfused spine at ALL segments C2-C3, C3-C4, C4-C5, C5-C6, and C6-C7.

T1 Acceleration Frontal Impact Model: For this loading condition, all nodes at or below the T1 vertebrae in the FE model were treated as a rigid body and loaded using four uniquely shaped acceleration pulses with identical ΔV's of 4.44 m/s and time intervals of 0.09 s (Figure 10). Frontal impact was simulated by accelerating the nodes in the anterior to posterior x-direction. The load was removed after it had run the full 92 ms duration and the body was allowed to continue its inertial movement until the

termination of the simulation at 300 ms. Data was outputted at 2.5 ms time intervals throughout the length of the simulation.

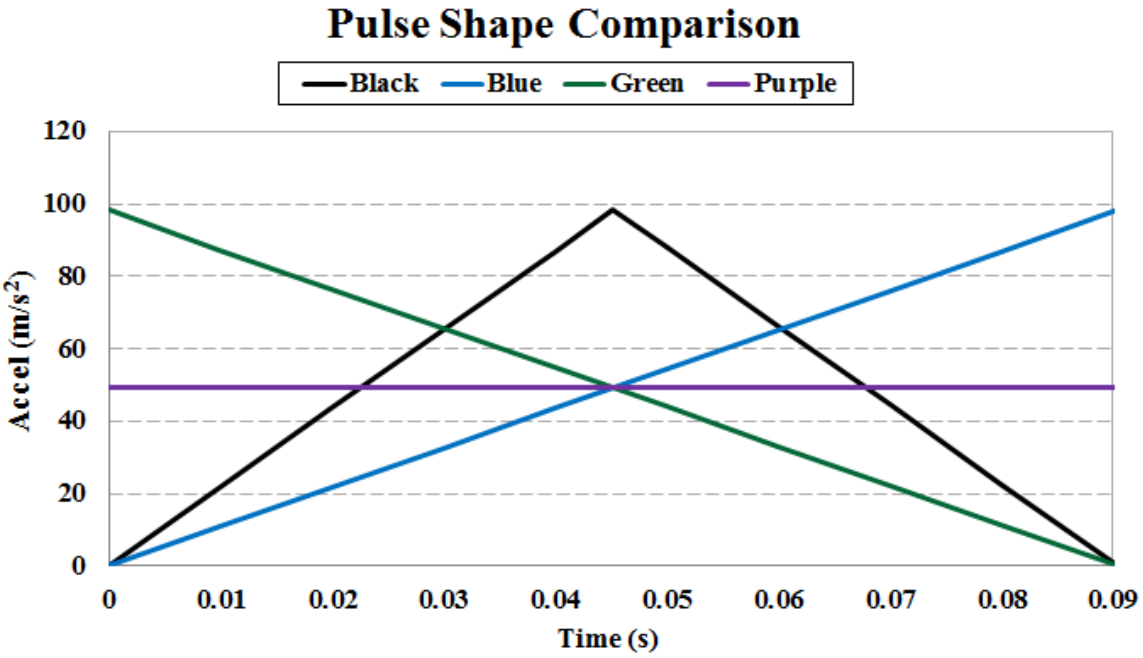

Figure 9: Different pulse shapes with the same ΔV of 4.44 m/s and same load interval of 92 ms.

T1 Acceleration Rear Impact Model: The T1 acceleration rear impact setup mimicked the frontal impact setup aside from one difference. Rear impact was simulated by accelerating the nodes at or below the T1 vertebrae in the posterior to anterior x-direction.

Seat Interaction Model: For the third loading condition, a seat and floor were added using rigid 4-by-4 element shells via LS-PrePost to the baseline THUMS model. The seat was defined as two separate parts: a seat back and a seat bottom. The seat angle was fit to the curvature of our validated FE model, and in accordance with the angles

described in SAE J826 H-point manikins fitted with a Head Restraint Measuring Device and the Euro NCAP whiplash testing protocol.[21,22]

Initially, the seat and floor were fixed in all 6 degrees of freedom (x-, y-, z- translational and x-, y-, z- rotational) and positioned 1 mm below the THUMS model. Gravity was then applied for 3 seconds to relax the THUMS model into the seat. The acceleration pulse was applied to both the seat and the floor in the posterior to anterior x-direction. Data was outputted every 2.5 ms.

3.3 Results

Tables 4 and 5 show the strains in the cervical spine ALL segments following a simulated T1 acceleration frontal impact and rear impact, respectively. In the frontal impact model, peak ALL strains ranged from 0.041 to 0.239. In the rear impact model, peak ALL strains ranged from 0.040 to 0.226. For both loading directions, strain did not vary at the C2-C3 level, and the greatest increase in strain (1.0%) was seen at the C6-C7 level.

Table 4: A comparison of ALL strains in the T1 Acceleration Frontal Impact model loaded with four differently shaped acceleration pulses.

ALL Segment	Black	Blue	Green	Purple
C2-C3	0.041	0.041	0.041	0.041
C3-C4	0.086	0.085	0.084	0.085
C4-C5	0.105	0.104	0.103	0.104
C5-C6	0.131	0.130	0.129	0.130
C6-C7	0.239	0.236	0.234	0.236

Table 5: A comparison of ALL strains in the T1 Acceleration Rear Impact model loaded with four differently shaped acceleration pulses.

ALL Segment	Black	Blue	Green	Purple
C2-C3	0.040	0.040	0.040	0.040
C3-C4	0.060	0.059	0.059	0.059
C4-C5	0.094	0.092	0.094	0.092
C5-C6	0.092	0.091	0.091	0.091
C6-C7	0.226	0.223	0.223	0.223

Table 6 shows the strains in the ALL following a simulated rear impact in the Seat Interaction model. Peak ALL strains ranged from 0.087 to 0.392. In general, the blue profile realized the lowest strains at each cervical level, followed by the purple and green profiles, respectively. The black pulse realized the highest strains at each cervical level. The greatest difference in strain (28.7%) was observed at the C2-C3 level between the blue and black pulses. The CPU runtime ranged from 4 to 7 hours per simulation. The runtime varied with two factors: CPU load and the number of cores used per simulation.

Table 6: A comparison of ALL strains in the Seat Interaction model loaded with four differently shaped acceleration pulses.

ALL Segment	Black	Blue	Green	Purple
C2-C3	0.112	0.087	0.106	0.101
C3-C4	0.152	0.123	0.138	0.132
C4-C5	0.206	0.167	0.197	0.181
C5-C6	0.212	0.168	0.212	0.198
C6-C7	0.392	0.344	0.376	0.356

3.4 Discussion

A complete human FE model was used to quantify the effects of pulse shape on strains in the ALL. In both T1 Acceleration models, the greatest difference in strain between any pair of identical ALL segments was 1.0%. This result supports our first hypothesis, suggesting that pulse shape has a negligible effect on strains in the ALL given a fixed ΔV and fixed time interval when the load is applied directly to the body.

However, the different curve contours produced significantly different strains at each ALL level when a vehicle seat was introduced to the FE model. This difference in strains supports our second hypothesis, and validates our use of the unique Euro NCAP

pulse in Chapter 2. In FE models built to simulate real-world vehicle impacts, the pulse shape contributes significantly to the resulting strains felt in the neck. The distinct profile of the employed Euro NCAP curve captures intricacies within the model that cannot be replicated by a simple square or triangular wave with the same ΔV and load time.

4. Conclusion

This thesis quantifies the effects of whiplash neck injury in scenarios wherein the occupant has previously undergone cervical or lumbar arthrodesis.

Three key points were drawn from the results in Chapter 2. In the models of cervical arthrodesis, peak ALL strains were found to be higher in the motion segments adjacent to the level of fusion compared to a healthy spine, and strains directly increased with longer fusions. C3-C4 appeared to be the motion segment at greatest biomechanical risk for adjacent segment strain following arthrodesis while C6-C7 showed high strain levels with little change following arthrodesis. Lumbar surgery had no statistical or clinically meaningful effect on the ALL strains in the cervical spine.

Two key points were observed from the results in Chapter 3. In the T1 Acceleration models, pulse shapes with identical ΔV's and load intervals produced nearly identical strains in the ALL. In the Seat Interaction model, the same pulse shapes outputted significantly different strains in the ALL.

Several limitations exist for future investigation but do not affect the conclusions drawn in this computational study. First, an expanded analysis may seek to address the roles of muscle and ligament contraction either in anticipation or as an instantaneous response to impact. Second, the current seat is represented as rigid and neither includes a head rest nor incorporate the whiplash prevention and mitigation technologies currently found in most vehicles. Third, the etiology of whiplash syndrome may involve

the facet capsules. However, the capsules are not modeled with sufficiently in v1.61 of the THUMS model for a confident strain analysis. These limitations do not change the conclusions made in this computational study.

References

1. Staff B. Blausen Gallery 2014. *Wikiversity Journal of Medicine* 2014.

2. Pashman R. Motion Preservation for the Cervical Spine [Spine Anatomy]. 2007. Available at: http://www.mspine.com/Spinal-Anatomy.htm, 2014.

3. Bridwell K. Ligaments [Spinal Anatomy]. 06/16/10, 2014. Available at: http://www.spineuniverse.com/anatomy/ligaments, 2014.

4. Bower AF. Introduction to Finite Element Analysis in Solid Mechanics [Applied Mechanics of Solids]. Available at: http://solidmechanics.org/Text/Chapter7_1/Chapter7_1.php, 2014.

5. van Ratingen M, Ellway J, Avery M, et al. The Euro NCAP Whiplash Test. *21st International Technical Conference on the Enhanced Safety of Vehicles*, 2009.

6. Eck JC, Hodges SD, Humphreys SC. Whiplash: a review of a commonly misunderstood injury. *The American journal of medicine* 2001;110:651-6.

7. Anderson SE, Boesch C, Zimmermann H, et al. Are There Cervical Spine Findings at MR Imaging That Are Specific to Acute Symptomatic Whiplash Injury? A Prospective Controlled Study with Four Experienced Blinded Readers. *Radiology* 2012;262:567-75.

8. Styrke J, Stålnacke B-M, Bylund P-O, et al. A 10-Year Incidence of Acute Whiplash Injuries After Road Traffic Crashes in a Defined Population in Northern Sweden. *PM&R*;4:739-47.

9. Curatolo M, Bogduk N, Ivancic PC, et al. The role of tissue damage in whiplash-associated disorders: discussion paper 1. *Spine* 2011;36:S309-15.

10. Yoganandan N, Cusick JF, Pintar FA, et al. Whiplash injury determination with conventional spine imaging and cryomicrotomy. *Spine* 2001;26:2443-8.

11. Jonsson H, Jr., Bring G, Rauschning W, et al. Hidden cervical spine injuries in traffic accident victims with skull fractures. *Journal of spinal disorders* 1991;4:251-63.

12. Taylor JR, Twomey LT. Acute injuries to cervical joints. An autopsy study of neck sprain. *Spine* 1993;18:1115-22.

13. Oglesby M, Fineberg SJ, Patel AA, et al. Epidemiological trends in cervical spine surgery for degenerative diseases between 2002 and 2009. *Spine* 2013;38:1226-32.

14. Schwab JS, Diangelo DJ, Foley KT. Motion compensation associated with single-level cervical fusion: where does the lost motion go? *Spine* 2006;31:2439-48.

15. Dang AB, Hu SS, Tay BK. Biomechanics of the anterior longitudinal ligament during 8 g whiplash simulation following single- and contiguous two-level fusion: a finite element study. *Spine* 2008;33:607-11.

16. Verma K, Gandhi SD, Maltenfort M, et al. Rate of Adjacent Segment Disease in Cervical Disc Arthroplasty Versus Single-Level Fusion: Meta-analysis of Prospective Studies. *Spine* 2013;38:2253-7 10.1097/BRS.0000000000000052.

17. Mertz HJ, Patrick LM. Investigation of the kinematics and kinetics of whiplash. *Proc. 11th STAPP Car Crash Conference*, 1967:SAE Paper No. 670919.

18. Ivancic PC, Pearson AM, Panjabi MM, et al. Injury of the anterior longitudinal ligament during whiplash simulation. *Eur Spine J* 2004;13:61-8.

19. Kitagawa Y, Yasuki T, Hasegawa J. A study of cervical spine kinematics and joint capsule strain in rear impacts using a human FE model. *Stapp car crash journal* 2006;50:545-66.

20. Group RCfARaIIWP. RCAR-IIWPG Seat/Head Restraint Evaluation Protocol. *Research Council for Automobile Repairs (RCAR) and International Insurance Whiplash Prevention Group (IIWPG). Version 2.5.*, 2006.

21. Programme ENCA. The Dynamic Assessment of Car Seats for Neck Injury Protection Testing Protocol (Version 3.1), 2011.

22. Society of Automotive Engineers I. Devices for use in defining and measuring vehicle seating accommodation. Warrendale, PA: SAE Publications, 1995.

23. Yoganandan N, Kumaresan S, Pintar FA. Geometric and mechanical properties of human cervical spine ligaments. *Journal of biomechanical engineering* 2000;122:623-9.

24. Bass CR, Lucas SR, Salzar RS, et al. Failure properties of cervical spinal ligaments under fast strain rate deformations. *Spine* 2007;32:E7-13.

25. Chen Y, He Z, Yang H, et al. Anterior cervical diskectomy and fusion for adjacent segment disease. *Orthopedics* 2013;36:e501-8.

26. Park JB, Cho YS, Riew KD. Development of adjacent-level ossification in patients with an anterior cervical plate. *The Journal of bone and joint surgery. American volume* 2005;87:558-63.

27. Siegmund GP, Sanderson DJ, Myers BS, et al. Awareness affects the response of human subjects exposed to a single whiplash-like perturbation. *Spine* 2003;28:671-9.

28. Siegmund GP, Blouin JS, Brault JR, et al. Electromyography of superficial and deep neck muscles during isometric, voluntary, and reflex contractions. *Journal of biomechanical engineering* 2007;129:66-77.

29. Siegmund GP, Myers BS, Davis MB, et al. Mechanical evidence of cervical facet capsule injury during whiplash: a cadaveric study using combined shear, compression, and extension loading. *Spine* 2001;26:2095-101.

30. Winkelstein BA, Nightingale RW, Richardson WJ, et al. The cervical facet capsule and its role in whiplash injury: a biomechanical investigation. *Spine* 2000;25:1238-46.